

Received July 2, 2020, accepted July 7, 2020, date of publication July 13, 2020, date of current version July 30, 2020.

Digital Object Identifier 10.1109/ACCESS.2020.3009039

# Real-Time Optimal Scheduling of Large-Scale Electric Vehicles: A Dynamic Non-Cooperative Game Approach

LVPENG CHEN<sup>ID</sup>, TAO YU<sup>ID</sup>, (Member, IEEE), YONGXIANG CHEN, WEILING GUAN, YING SHI, AND ZHENNING PAN<sup>ID</sup>

School of Electric Power Engineering, South China University of Technology, Guangzhou 510640, China

Corresponding author: Zhenning Pan (scutpanzn@163.com)

This work was supported in part by the National Natural Science Foundation of China under Grant 51777078.

**ABSTRACT** In the presence of the increasing penetration of electric vehicles (EVs) and conflict of independent optimization objectives among each electric vehicle aggregator (EVA), real-time optimal scheduling (RTOS) of large-scale EVs based on dynamic non-cooperative game approach is proposed for optimal decision makings in a dynamic pricing market. First, real-time optimal scheduling framework is designed to describe the flow of energy and information. Then, equivalent model of large-scale EVs is formulated to address “curse of dimensionality” caused by a large number of decision variables. Then, the potential game theory is used to study the existence and uniqueness of the Nash equilibrium (NE) solution. Finally, a distributed approach based on alternating direction method of multipliers (ADMM) is designed to achieve the equilibrium. Case studies demonstrate that the proposed approach achieves peak load shifting and reduces cost of EVAs significantly. Furthermore, the proposed method obtains higher-quality solution compared with other methods and is more applicable for real-time optimal scheduling of large-scale EVs due to its high computation efficiency and privacy protection.

**INDEX TERMS** Large-scale electric vehicles, real-time optimal scheduling, dynamic non-cooperative game, distributed optimization.

## NOMENCLATURE

### A. SETS

$\mathcal{N}$  set of EVAs  $\{1, \dots, N\}$   
 $\mathcal{T}$  set of time slots  $\{1, \dots, T\}$   
 $\mathcal{K}_t$  set of time slots  $\{t, \dots, T\}$   
 $\mathcal{K}'_t$  set of time slots  $\{t+1, \dots, T\}$

### B. VARIABLES

$E_{EV}(t)$  cumulative energy trajectory of EV at time-slot  $t$   
 $P_{EV}(t)$  charging power of EV at time-slot  $t$   
 $P_{\min}(t)$  minimum allowed charging power of EV at time-slot  $t$   
 $P_{\max}(t)$  maximum allowed charging power of EV at time-slot  $t$   
 $E_m(t)$  cumulative energy trajectory of EVC  $m$  at time  $t$

$E_{\min,m}(t)$  lower cumulative energy trajectory boundary of EVC  $m$  at time-slot  $t$   
 $E_{\max,m}(t)$  upper cumulative energy trajectory boundary of EVC  $m$  at time-slot  $t$   
 $P_m(t)$  charging power of EVC  $m$  at time-slot  $t$   
 $P_{i,m}(t)$  charging power of EVC  $m$  in EVA  $i$  at time-slot  $t$   
 $P_{\min,m}(t)$  minimum allowed charging power of EVC  $m$  at time-slot  $t$   
 $P_{\max,m}(t)$  maximum allowed charging power of EVC  $m$  at time-slot  $t$   
 $P_{\min,m,l}(t)$  minimum allowed charging power of  $l$ th EV in EVC  $m$  at time-slot  $t$   
 $P_{\max,m,l}(t)$  maximum allowed charging power of  $l$ th EV in EVC  $m$  at time-slot  $t$   
 $C_i(t)$  electricity purchasing cost of EVA  $i$  at time-slot  $t$   
 $p(t)$  dynamic electricity price at time-slot  $t$   
 $Q_i(t)$  electricity purchasing quantities of EVA  $i$  at time-slot  $t$

The associate editor coordinating the review of this manuscript and approving it for publication was Huai-Zhi Wang<sup>ID</sup>.

$Q_{i,m}(t)$	electricity purchasing quantities of EVC $m$ in EVA $i$ at time-slot $t$
$U_i(t)$	user group satisfaction of EVA $i$ at time-slot $t$
$F_{i,t}$	self-optimization objective function of EVA $i$ at time-slot $t$
$Q_{\text{total}}(t)$	total electricity supply of DSO at time-slot $t$
$Q_{\text{sum}}(t)$	sum of electricity purchasing quantities of all EVAs at time-slot $t$
$p(t)$	electricity price at time-slot $t$
$x(t)$	decision vector of all EVAs
$x_i(t)$	decision vector of EVA $i$ at time-slot $t$
$x_{-i}(t)$	decision vector of all EVAs other than EVA $i$ at time-slot $t$
$x^{\text{NE}}(t)$	Nash equilibrium solution of all EVAs at time-slot $t \{x_i^{\text{NE}}(t), i \in N\}$
$x_i^{\text{NE}}(t)$	Nash equilibrium solution of EVA $i$ at time-slot $t$
$x_{-i}^{\text{NE}}(t)$	Nash equilibrium solution of all EVAs other than EVA $i$ at time-slot $t$
$X_i(t)$	decision vector space of the EVA $i$ at time-slot $t$
$P(x(t))$	potential function

### C. PARAMETERS

$E_{\min}(t)$	lower cumulative energy trajectory boundary of EV at time-slot $t$
$E_{\max}(t)$	upper cumulative energy trajectory boundary of EV at time-slot $t$
$\eta$	efficiency of charging
$\Delta t$	time interval
$t_{\text{arr}}, t_{\text{dep}}$	arrival and departure time of EV
$E_{\text{exp}}$	expected charging demand of EV
$P_{\text{EV,max}}$	maximum allowed charging power of EV
$n_{m,t}$	number of EVs in EVC $m$ at time-slot $t$
$E_{\min,m,l}(t)$	lower cumulative energy trajectory boundary of the $l$ th EV in EVC $m$ at time-slot $t$
$E_{\max,m,l}(t)$	upper cumulative energy trajectory boundary of the $l$ th EV in EVC $m$ at time-slot $t$
$M_k$	number of EVC at time-slot $t$
$\omega_i(t)$	satisfaction morphological parameter of EVA $i$ at time-slot $t$
$\lambda_i$	satisfaction coefficient of EVA $i$ at time-slot $t$
$Q_{\max,i,m}(t)$	maximum allowed electricity quantities of EVC $m$ in EVA $i$ at time-slot $t$
$Q_{\text{load}}(t)$	conventional load profile at time-slot $t$
$N$	number of EVAs under control of DSO
$\delta(t)$	electricity price coefficient at time-slot $t$
$p_{\text{max}}$	maximum allowed electricity price
$Q_{\text{max}}$	maximum allowed power supply of the DSO
$T$	number of total scheduling periods
$\rho$	penalty coefficient
$u$	Lagrangian multiplier

### D. INDICES

$t$	index of scheduling periods
$z$	index of iterations

### E. ABBREVIATIONS

EV	electric vehicle
EVA	electric vehicle aggregator
EVC	electric vehicle cluster
RTOS	real-time optimal scheduling
DSO	distributed system operator
MPC	model predictive control
NE	Nash equilibrium
ADMM	alternating direction method of multipliers

### I. INTRODUCTION

Electric vehicle (EV) has attracted enormous attentions around the world with its significant advantages in low pollution emission and energy saving [1]–[3]. So far, many countries have promoted the deployment of EV [4], e.g., United States, China, and Japan.

Under the increasing EV penetration, the uncoordinated scheduling of large-scale EVs challenges the reliable and economic operation of power system [5], e.g., transformer overloading and voltage violation. However, coordinated scheduling of large-scale EVs can assist in automatic generation control or integrated energy system dispatch [6], [7]. Thus, real-time optimal scheduling (RTOS) of large-scale EVs has attracted significant attentions in recent years for its remarkable performance of peak load shifting and cost saving. Typically, real-time coordination of EV charging was studied to minimize power losses and improve voltage profile in [8]. RTOS for parking lots considering the renewable resources was presented in [9]. RTOS for electric vehicle aggregator (EVA) in a market environment was studied in [10]. A convex quadratic programming framework for RTOS is proposed to reduce the computing time in [11].

However, the aforementioned studies consider explicit single EV model in optimization, which leads to enormous computation and large data communication when large scale EVs access to the power system. It is more complex to perform RTOS than day-ahead optimal scheduling with large scale EVs access, because the behavior characteristics of EVs are highly random and speed of computation must be fast enough to meet the real-time requirement [12].

To apply RTOS of large-scale EVs, there are the following three issues should be considered:

1) High bandwidth data communication requirement and the “curse of dimensionality” caused by traditional single EV modeling with the increasing EV penetration.

2) Systematic uncertainty: including factors such as EV owner behavior, EV information differences, and forecast accuracy of future EV arrival and so on [13].

3) Sequential decision-making: since the decision-making of RTOS in a certain period of time needs to consider the system changes in multiple stages in the future. EV charging incorporates temporally coupled SOC constraints. Thus, the impacts of current decision to the future have to be considered.

To tackle the above-mentioned challenges, equivalent model of large-scale EVs is introduced to address “curse of dimensionality” problem [14], [15]. In [14], individual EV charging constraints were aggregated upwards in a tree structure. In [15], the cumulative charging energy and power boundaries of all EV were aggregated. Besides, model predictive control (MPC) is the most widely used method to address uncertainty and sequential decision-making problem. For example, in [16] and [17], using the historical data, MPC was adopted to clear the real-time transactive market by assuming the future responses are known [18].

At present, the existing research focused on RTOS is usually from the grid-side perspective and adopts centralized algorithm to achieve the optimal operation [19], [20]. However, in the scenario of electricity market, EVA becomes the independent agent to individually make decision [21] and lay emphasis on protecting its commercial privacy data [22]. Therefore, it is necessary to consider the dynamic non-cooperative scheduling among EVAs.

So far, game theory has been gradually applied to EV optimal scheduling [23]–[25]. Reference [23] used Stackelberg game to maximize the benefits of EVA and EV owners. However, uncertainties of EV behaviors were not considered. Reference [24] proposed a cooperative and non-cooperative optimal scheduling model based on robust Stackelberg game considering the uncertain charging demand. Reference [25] proposed an optimal scheduling for EVs based on dynamic non-cooperative game. However, all the above-mentioned works study day-ahead scheduling and are difficult to be applied in RTOS. Besides, the above research is based on a single EV as an optimized unit, which is not suitable for large-scale EVs.

In view of the shortcomings of the existing research, this paper studies RTOS of large-scale EVs based on dynamic non-cooperative game. The main contributions of this paper are summarized as follows:

- A dynamic non-cooperative game approach is introduced to RTOS of large-scale EVs. The existence of the unique Nash equilibrium (NE) solution is proved by the exact potential game theory.
- The centralized optimal problem is decomposed and solved by distributed algorithm based on ADMM, thus the optimal real-time solution can be rapidly made by each EVA.
- A RTOS of large-scale EVs based on MPC and the equivalent model of large-scale EVs are developed to avoid “curse of dimensionality” and reduced the computing complexity. The computing time is short and

grows slowly as number of EV and EVA increases, thus it is applicable to RTOS of extremely large-scale EVs.

The remaining of this paper is organized as follows. Section II designs the framework of RTOS. Section III introduces the optimization problem formulation. Section IV introduces an improved solution method. Case studies are carried out in Section V. Finally, Section VI briefly summarizes the paper.

## II. FRAMEWORK OF REAL-TIME OPTIMAL SCHEDULING

The framework of RTOS is designed in this paper. As shown in Fig. 1. The framework consists of two entities, i.e., distributed system operator (DSO) and EVA. DSO supplies electricity to all EVAs and conventional load within its jurisdiction, and coordinates the charging plan of all EVAs. EVA develops a charging plan to minimize its own costs (maximize its own revenues), which needs to consider the status of EVs that have arrived at present and will arrive in the future. There are various forms of EVA, e.g., stand-alone EV charging stations, parking lots of large shopping mall with charging piles, or a collection of all distributed household charging piles in a certain area.

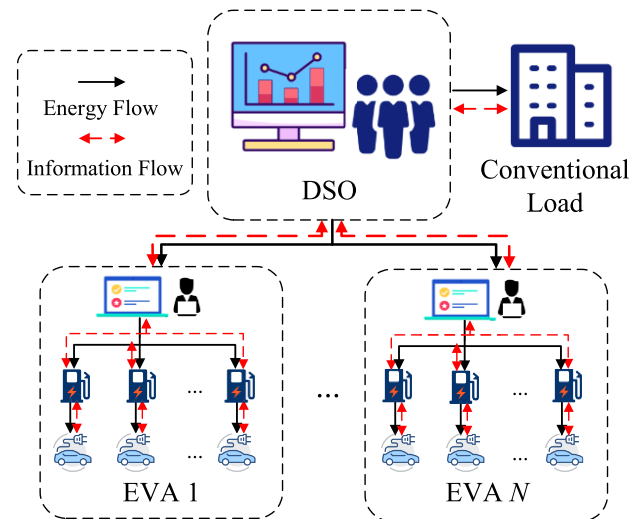


FIGURE 1. Framework of real-time optimal scheduling.

With the help of high-speed communication means such as 5G network and optical fiber communication, DSO broadcasts dynamic electricity price to EVAs in real-time in order to guide EVAs to transfer the charging load from high consumption period to low consumption period. At the same time, DSO receives the charging plan of all EVAs, and considers the predicted information of the conventional load in the area to adjust the dynamic electricity price in real-time [26], [27]. After receiving the dynamic electricity price, EVAs will update their charging plans considering their own optimization target and EV information and then, upload the updated plan back to DSO. The cycle will continue until the power is balanced.

### III. PROBLEM FORMULATION

#### A. EV MODELING

The mathematical model of EV model can be described as:

$$\begin{cases} E_{EV}(t) = E(t_{arr}) + \eta \sum_{k=t_{arr}}^t P_{EV}(k)\Delta t \\ = E(t-1) + \eta P_{EV}(t)\Delta t \\ E_{min}(t_{dep}) = E_{max}(t_{dep}) = E_{exp} \\ E_{min}(t) \leq E_{EV}(t) \leq E_{max}(t) \\ P_{max}(t) = \min \left( P_{EV,max}, \frac{E_{max}(t) - E(t-1)}{\eta\Delta t} \right) \\ P_{min}(t) = \max \left( 0, \frac{E_{min}(t) - E(t-1)}{\eta\Delta t} \right) \\ P_{min}(t) \leq P_{EV}(t) \leq P_{max}(t) \end{cases} \quad (1)$$

where the charging power of each EV is maintained constant during each time-slot. Therefore, the flexibility of EV can be represented by its cumulative energy boundaries.

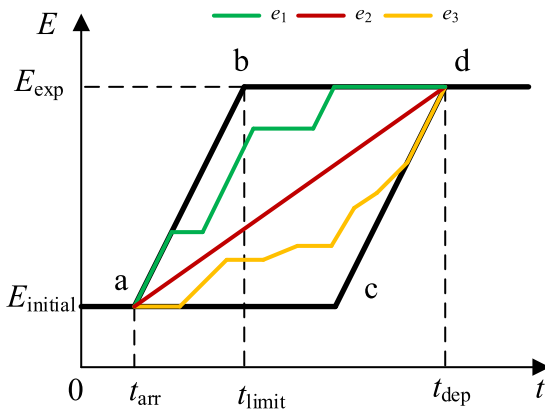


FIGURE 2. Cumulative energy boundaries modeling of EV.

As shown in Fig.2, an EV with expected charging demand  $E_{exp}$  arrives at  $t_{arr}$  and departs at  $t_{dep}$ . The curve a-b-d is the upper cumulative energy boundary  $E_{max}(t)$ , indicating that EV is instantaneously charged at the maximum charging power after arriving at the EVA until its cumulative energy trajectory  $E_{EV}(t)$  reaches the  $E_{exp}$ . While the curve a-c-d is the lower cumulative energy boundary  $E_{min}(t)$ , indicating that charging is delayed after arriving at the EVA as long as possible without charging demand loss. The slope of the lines a-b and c-d equals to the maximum practical charging power  $\eta P_{EV,max}$ .

$$t_{limit} = t_{arr} + \frac{E_{exp} - E_{initial}}{\eta P_{EV,max}} \quad (2)$$

For a single EV, a single EV energy boundary model exhibits a “parallelogram” configuration. In general, the longer the EV is connected to the EVA, the stronger its adjustable capability is, the wider the model shape is, and the narrower the opposite. In general, the residence time of EV at EVA determines its schedulability.  $t_{limit}$  is the boundary charging time to distinguish whether the charging scheduling

of EV is available. When the EV owner sets the  $t_{dep}$  less than  $t_{limit}$ , the EV does not have the schedulability.

#### B. EQUIVALENT MODEL OF ELECTRIC VEHICLE CLUSTER

In order to overcome “curse of dimensionality” caused by large-scale EVs, EVs with the same departure time which is set by the EV owner are classified into the same electric vehicle cluster (EVC). Based on the EV modeling of EVs in the same EVC, the equivalent models of EVCs can be described as:

$$\begin{cases} E_m(t) = \eta \sum_{k=1}^t P_m(k)\Delta t = E_m(t-1) + \eta P_m(t)\Delta t \\ E_{min,m}(t) = \sum_{l=1}^{n_{m,t}} E_{min,m,l}(t) \\ E_{max,m}(t) = \sum_{l=1}^{n_{m,t}} E_{max,m,l}(t) \\ E_{min,m}(t) \leq E_m(t) \leq E_{max,m}(t) \\ P_m(t) = \sum_{l=1}^{n_{m,t}} P_{m,l}(t) \\ P_{min,m}(t) = \sum_{l=1}^{n_{m,t}} P_{min,m,l}(t) \leq P_m(t) \\ P_{max,m}(t) = \sum_{l=1}^{n_{m,t}} P_{max,m,l}(t) \geq P_m(t) \end{cases} \quad (3)$$

*Remark 1:* Equivalent model of EVC is equivalent to the large-scale EVs, which indicates that there always exists at least one reallocation strategy satisfying Eq.(1) if the charging power of EVC meets Eq.(3). (Detailed proof can be found in [28]).

Note that  $E_{min,m}(t)$ ,  $E_{max,m}(t)$ ,  $P_{min,m}(t)$  and  $P_{max,m}(t)$  of EVC  $m$  (for  $m \in \mathcal{K}_t$ ) can be calculated by EVA according to the real-time information of arrived EVs, while  $E_{min,m}(k)$ ,  $E_{max,m}(k)$ ,  $P_{min,m}(k)$ , and  $P_{max,m}(k)$  of EVC  $m$  (for  $m \in \mathcal{K}_t$  and  $k \in \mathcal{K}'_t$ ) need to be forecasted based on historical information and some real-time information. Introducing the equivalent model of EVC can reduce and fix the number of decision variables in the RTOS, which means that the scale of EVs does not affect the number of decision variables and the “curse of dimensionality” can be avoided after EV large-scale access.

#### C. OBJECTIVE FUNCTION OF EVA

In the current time-slot  $t$ , EVA  $i$  aims to minimize the value of its own objective function, which includes the payment to the PSO over time period  $\mathcal{T}$  minus the satisfaction of the EV owners. Higher charging satisfaction helps EVA reduce user churn and increase its long-term benefits. The EV owners hope that their EVs can be charged as early as possible to meet their next travel (especially when the owners need to use EVs in advance with sufficient power). The objective function of EVA can be obtained as:

$$\min F_i = \mathbf{E} \left( - \sum_{t=1}^T U_i(t) + \sum_{t=1}^T C_i(t) \right) \quad (4)$$

$$C_i(t) = p(t)Q_i(t) = p(t) \sum_{m=t+1}^{|\mathcal{K}'_t|} Q_{i,m}(t) \quad (5)$$

$$U_i(t) = \omega_i(t) \sum_{m=t+1}^{|\mathcal{K}'_t|} (-Q_{i,m}^2(t) + 2Q_{max,i,m}(t)Q_{i,m}(t)) \quad (6)$$

$$Q_{i,m}(t) = P_{i,m}(t) \cdot \Delta t \quad (7)$$

$$\omega_i(t) = \frac{t}{T} \lambda_i \quad (8)$$

where  $\mathbf{E}$  is the desired operator;  $\omega_i(t)$  is in  $\$/(\text{kW} \cdot \text{h})^2$  or  $\$/(\text{MW} \cdot \text{h})^2$  which is monotonically increasing and non-negative;  $\lambda_i$  indicates the importance of each EVA to user satisfaction.

Note that it is difficult to solve or calculate Eq.(4) directly, due to the system state of EVA in the future time is unclear at the current time-slot  $t$ . Therefore, the MPC theory is introduced to deal with the uncertain problems in future time. The objective function of EVA can be converted into new form and divided into two parts(current time and future), which can be expressed as:

$$\min F_{i,t} = -U_i(t) + C_i(t) - \sum_{\tau=t+1}^T U_i(\tau) + \sum_{\tau=t+1}^T C_i(\tau) \quad (9)$$

At each optimization time-slot  $t$ , EVA makes the optimization decision over time period  $\mathcal{K}_t$  based on the known information and forecasting information, but only the first part of decision(current time-slot  $t$ ) can be adopted to schedule large-scale EVs.

#### D. DYNAMIC ELECTRICITY PRICE SCHEME

The DSO is responsible for providing power to the conventional load and all EVAs in real time. Therefore, the total power supply from DSO and the total power requirement of all EVAs can be expressed as:

$$Q_{\text{total}}(t) = Q_{\text{load}}(t) + Q_{\text{sum}}(t) \quad (10)$$

$$Q_{\text{sum}}(t) = \sum_{i=1}^N Q_i(t) \quad (11)$$

The aim of DSO is to perform the peak load shifting and production cost reducing. By adopting a reasonable dynamic electricity price scheme, EVA is motivated to shift the charging load from the peak of the system load to the bottom, which not only reduces the peak-to-valley difference of the system load, but also reduces the risk of grid operation. For example, in the period of high load, high electricity price can be set to suppress the charging desire of each EVA, so the risk of exceeding the capacity of the transformer can be avoided, and the peak clipping effect can be achieved. In the period of low load, the transformer capacity is sufficient, so the low electricity price can be set to stimulate EVAs. Generally speaking, DSO has to set the dynamic electricity price based on the load ratio of the transformer [29]. A common dynamic electricity price scheme can be expressed as:

$$p(t) = \delta(t) \cdot Q_{\text{total}}(t) \quad (12)$$

$$\delta = \frac{1}{Q_{\text{max}}} p_{\text{max}} \quad (13)$$

where  $p_{\text{max}}$  is set by the DSO based on the government policies limit or the practical experience of the grid.

## IV. SOLUTION METHODOLOGY

### A. DYNAMIC NON-COOPERATIVE GAME MODEL

According to the dynamic electricity price provided from DSO, considering their own benefits, EVAs will actively adjust their charging plans to minimize their own value of objective function. In addition, each EVA is competitive with each other and has no cooperative relationship with each other, which indicates that the game model proposed in this paper is a dynamic non-cooperative game model.

According to the non-cooperative game theory, each EVA is regarded as an individual rational and selfish game player, and there is no direct connection and no mutual restraint agreement among them. In the process of dynamic game, each EVA always pursue the minimum of value of objective function. Therefore, the interaction among EVAs can be described as the follow:

**Game 1:** EVAs' Dynamic Non-cooperative Game:

1) **Players:** All EVAs within the jurisdiction of the DSO;

2) **Strategies:** The strategy of EVA  $i$  at the time-slot  $t$  is  $x_i(t)$ ;  $x_{-i}(t)$  is the strategy set removing the strategy of EVA  $i$ ;  $x(t) = \{x_i(t), i \in \mathcal{N}\} = \{x_i(t), x_{-i}(t)\}$  is the strategy set of all EVAs;  $X_i(t)$  is the decision space of EVA  $i$  at the time-slot  $t$ .

3) **Payoffs:** It can be known from Eqs.(10)-(13) that the dynamic electricity price is a function of the total electricity consumption. Therefore, payoff of the each EVA can be expressed as  $F_{i,t}(x_i(t), x_{-i}(t))$ .

According to the definition of NE, at the current scheduling time-slot  $t$ ,  $x^{\text{NE}}(t) = \{x_i^{\text{NE}}(t), i \in \mathcal{N}\}$  is the NE solution of the game. By adopting this strategy, all EVAs have no intention to modify their own strategies unilaterally, i.e., for  $\forall x_i(t) \in X_i(t)$ ,

$$F_{i,t}(x_i(t), x_{-i}^{\text{NE}}(t)) \geq F_{i,t}(x_i^{\text{NE}}(t), x_{-i}^{\text{NE}}(t)), \quad i \in \mathcal{N} \quad (14)$$

Therefore, the NE solution can be considered as the solution to the optimization problem of each EVA when other EVAs' strategies are fixed as NE solution:

$$\min_{x_i(t) \in X_i(t)} F_{i,t}(x_i(t), x_{-i}^{\text{NE}}(t)), \quad i \in \mathcal{N} \quad (15)$$

### B. EXACT POTENTIAL GAME

In general, it is a difficult task to proof the existence of a pure strategy NE in a game. However, Game 1 can be regarded as an exact potential game. According to the characteristics of exact potential game, the existence of NE strategy can be guaranteed [30]. The definition is given as follow:

*Definition:* A game can be regarded as an exact potential game if there is a function  $P(x(t))$  for all  $i \in \mathcal{N}$  and strategies  $(x'(t), x_{-i}(t))$  and  $(x(t), x_{-i}(t))$ , there is:

$$\begin{aligned} P(x'_i(t), x_{-i}(t)) - P(x_i(t), x_{-i}(t)) \\ = F_i(x'_i(t), x_{-i}(t)) - F_i(x_i(t), x_{-i}(t)) \end{aligned} \quad (16)$$

Equation indicates that the change in the potential function equals to the unilateral change in the payoff of an individual EVA, i.e., the potential function can completely reflect the change in the payoffs of the players.

*Remark 2:* Game 1 is an exact potential game, and its potential function can be constructed as follow:

$$\begin{cases} P(x(t)) = P_1(x(t)) + P_2(x(t)) \\ P_1(x(t)) = - \sum_{i \in \mathcal{N}} \sum_{k \in \mathcal{K}} U_i(k) \\ P_2(x(t)) = \sum_{i \in \mathcal{N}} \left[ \sum_{k \in \mathcal{K}} (\delta(k) Q_{\text{load}}(k) Q_i(k) \right. \\ \left. + \delta(k) Q_i^2(k) + \sum_{i < j \in \mathcal{N}} \delta(k) Q_i(k) Q_j(k) \right] \end{cases} \quad (17)$$

The correctness of construction can be proved in Appendix A. In addition, we prove that  $P(x(t))$  is a convex function of  $x(t)$  and feasible space is convex in Appendix B. According to the characteristics of the potential game, the unique NE solution of the potential game is mapped onto the global minimum point of the corresponding potential function. Therefore, solving the game model proposed in this paper is equivalent to finding the global minimum point of the potential function.

### C. DISTRIBUTED REAL-TIME SOLUTION METHOD BASED ON ADMM

It is available to solve the exact potential game model by a centralized approach. However, centralized approach is not suitable to apply in RTOS with gaming situation, which requires high communication bandwidth, fast computing power, and high level of privacy protection of EVAs. Distributed approach is introduced to enable each EVA to solve its own optimization problem using local information and update a little bit of information to advance the iteration, which protect the privacy of EVAs and reduced communication bandwidth and computing requirements. In this paper, the model is solved by the ADMM algorithm with good convergence and adaptability. It should be pointed out that other distributed algorithms can also be applied to solve the model [31], [32].

*Remark 3:* The potential function in Eq.(17) can be decomposed by variables into independent sub-optimization problems of DSO and each EVA, as shown as follow:

$$\begin{cases} W_1(Q_{\text{sum}}) = \frac{1}{2} \sum_{k \in \mathcal{K}} \delta(k) Q_{\text{sum}}^2(k) \\ + \sum_{k \in \mathcal{K}} \delta(k) Q_{\text{load}} Q_{\text{sum}}^2(k) \\ W_2(Q_i, U_i) = - \sum_{k \in \mathcal{K}} U_i(k) + \frac{1}{2} \sum_{k \in \mathcal{K}} \delta(k) Q_i^2(k) \end{cases} \quad (18)$$

where  $W_1$  and  $W_2$  are sub-optimization problems of DSO and each EVA, respectively; The proof of decomposition process can be found in Appendix C.

Referring to [33], the iteration of each decision variable in the ADMM algorithm can be expressed as:

$$\begin{cases} Q_{\text{sum}}^{(z+1)} = \arg \min(W_1(Q_{\text{sum}}) \\ + \frac{\rho}{2} \|Q_{\text{sum}} - Q_{\text{sum}}^{(z)} + \bar{Q}^{(z)} + u^{(z)}\|^2) \\ Q_i^{(z+1)} = \arg \min(W_2(Q_i, U_i) \\ + \frac{\rho}{2} \|-Q_i + Q_{\text{sum}}^{(z)} + \bar{Q}^{(z)} + u^{(z)}\|^2) \\ u^{(z+1)} = \bar{Q}^{(z)} + u^{(z)} \\ \bar{Q}^{(z+1)} = \frac{1}{N+1}(Q_{\text{sum}}^{(z+1)} + \sum_{i \in \mathcal{N}} Q_i^{(z+1)}) \end{cases} \quad (19)$$

The convergence criterion of the ADMM algorithm is that the primal infeasibility and the dual infeasibility are less than the convergence precision. For more detailed of specific formula derivation and the proof of the convergence of the ADMM algorithm, readers can refer to [33].

### D. DISTRIBUTED REAL-TIME OPTIMIZATION PROCESS

A scheduling algorithm that can be executed by DSO and EVAs is proposed. The algorithm involves the initiation and scheduling phases, which are presented in Algorithm 1.

---

#### Algorithm 1 Scheduling Algorithm in Time-Slot $t$

---

- **Initiation phase**

**If**  $t = 0$

DSO and EVAs randomly initialize strategy profile  $x^{(1)}(t)$ .

Based on the complete prediction information, EVAs initialize the boundary information of each EVC by Eq.(2).

**Else**

DSO and EVAs initialize strategy profile  $x^{(1)}(t)$  by the NE strategy  $x^{\text{NE}}(t-1)$  in the previous time-slot  $t-1$ .

Based on the prediction information and accessed EVs information, EVAs update the boundary information of each EVC by Eq. (2).

**End if**

- **Scheduling phase**

**Repeat**

DSO and each EVA solve their own optimization problem and update the strategy  $x^{(z)}(t)$  by Eq. (18).

EVAs upload the charging strategy information to DSO.

DSO updates the unbalance magnitude and the lagrangian multiplier by Eq.(18), and broadcasts them to EVAs.

$z=z+1$

**Until** convergence conditions are satisfied

EVAs allocate their own managed EVs charging strategies

---

## V. CASE STUDIES

### A. PARAMETER SETTINGS

The optimization horizon starts from 7:00 am and ends at 7:00 am the next day, and the simulation time interval  $\Delta t$  is

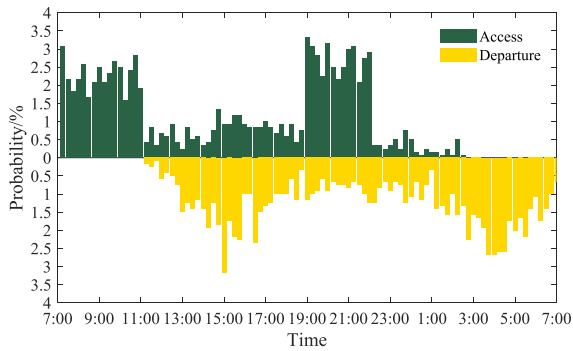


FIGURE 3. The driving patterns of the EV owners.

15 min, which means that the horizon is divided into  $T = 96$  time-slots. The charging scenarios involve 3 EVAs and 1200 EVs unless otherwise specified. Each EV selects one of the EVAs to be charged randomly. The driving patterns of the EV owners are shown in Fig.3. Three types of EV are considered whose characteristic parameters are shown in TABLE 1. Assuming that all the owners of the EVs expect that the EV battery can be fully charged before departure time  $t_{out}$ . The charging efficiency  $\eta$  is set to be 99%.  $\lambda_i$  is set to be  $0.003\$/(\text{kWh})^2$ .  $\delta(t)$  is set to be  $0.204\$/\text{MWh}$ .  $SOC_{initial}$  is assumed to follow the normal distribution  $N(0.5, 0.1^2)$ . The convergence criterion of ADMM algorithm is set to  $10^{-3}$ . The forecasting error of the conventional load is not considered.

TABLE 1. EV characteristic parameters in simulation.

Number of EVA	EV battery capacity/kWh	EV charging limit/kW	Ratio/%
3	24	4	30
	36	6	40
	48	8	30

All simulations are modeled in MATLAB R2017a using a PC with inter(R) Core(TM) i7-6700 3.40GHz, and 16G memory. Each sub-problem is solved by CPLEX toolbox in GAMS.

**B. PERFORMANCE OF OPTIMIZATION MODEL**

In this section, the optimization result of the proposed model is shown in Fig.4, compared with conventional load curve and disordered charging curve (i.e., EVs are charged at the maximum charging power after arriving at EVA).

It can be seen that the conventional load has two peaks of electricity consumption at noon and at night, since large-scale of EVs arrive at EVAs to start charging during these periods. This situation will increase the peak-valley difference of the system, and raise the risk of system operation. By adopting the proposed model, the peak-valley difference is 8.77% lower than that of disordered charging.

**C. EQUIVALENCE VERIFICATION OF DISTRIBUTED OPTIMIZATION**

Fig.5 and Fig.6 compares the results and the value of objective function between distributed and centralized optimal scheduling methods at each time-slot, respectively. It can

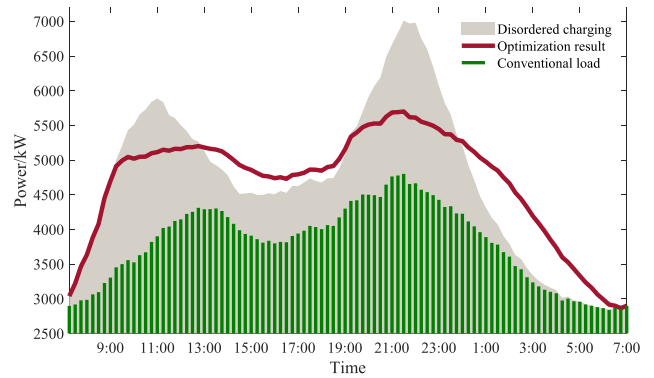


FIGURE 4. Performance of optimization model.

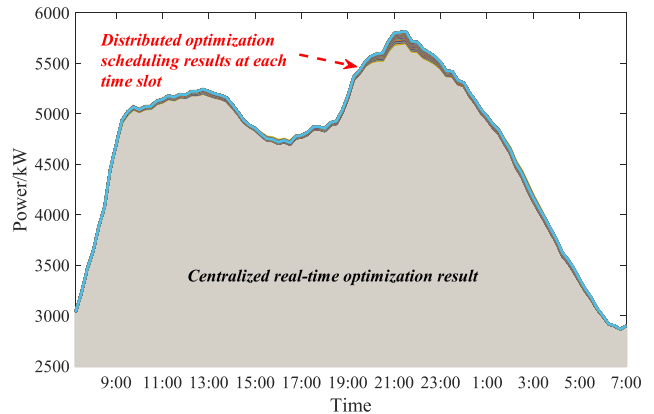


FIGURE 5. Comparisons of distributed and centralized optimal scheduling results at each time slot.

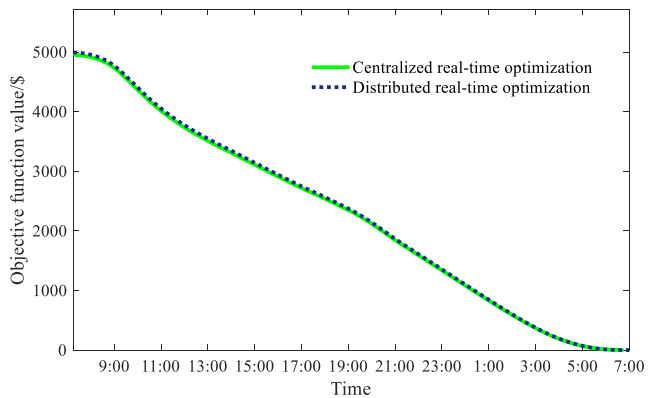


FIGURE 6. Objective function comparison of the decentralized model and the centralized model at each time-slot.

be seen that the results of the distributed and centralized scheduling method are basically consistent, which indicates that the equivalence of the distributed optimization method and correctness of the decomposition process are verified. So the distributed and centralized optimal scheduling method are equivalent at each time-slot within the allowable error.

In addition, the privacy security of DSO and EVAs can be guaranteed by using distributed real-time solution method, because the communication information between the DSO

and each EVA is only overall charging strategies, Lagrangian multiplier and other few information, whose size is very small. It is very easy to transmit information by using high-speed communication means such as 5G network and optical fiber.

**D. APPLICATION FEASIBILITY VERIFICATION**

The convergence speed of the distributed algorithm determines whether the model can be practically applied in engineering. Fig.7 and Fig.8 show the variation of the primal feasibility and the dual feasibility at each optimization time-slot, respectively. It can be seen that at most of the time-slots during the RTOS, convergence can be achieved through around 40 to 55 times (average iteration number is about 49 times). Note that since the iterative initial point of the time-slot 1 is arbitrarily chosen, the calculation speed of time-slot 1 are slow with 541 iteration times to reach convergence. However, it is possible to deal with this problem by adopting a day-ahead scheduling in advance to obtain an initial iteration point which is close to the optimal solution of RTOS.

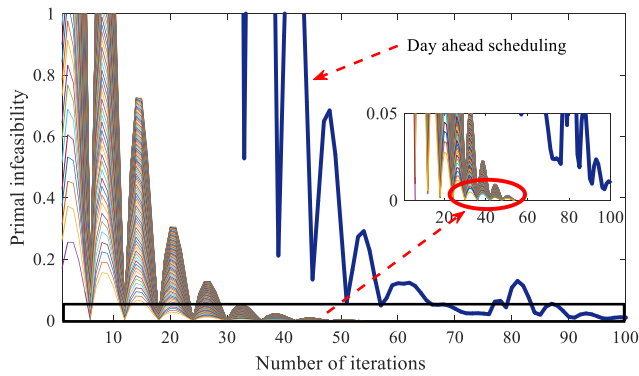


FIGURE 7. Convergence curve of primal feasibility.

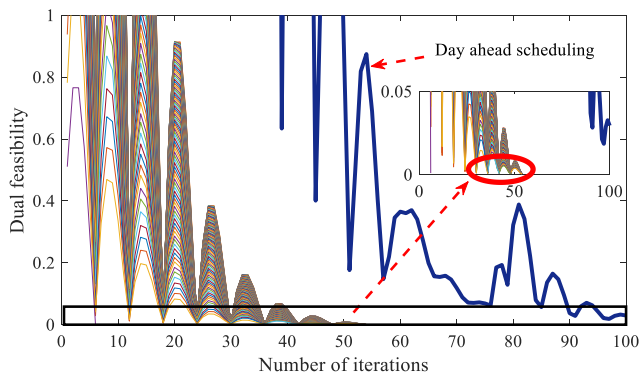


FIGURE 8. Convergence curve of dual feasibility.

After simulation, the maximum time of each sub-problem at each iteration does not exceed 0.58s (average time is 0.43s) In practical engineering applications, assuming that the communication delay is 0.05s and parallel computing is adopted by DSO and EVAs, optimization solving of each

time-slot can be done within 24s. To conclude, the model and algorithm can meet the requirements of rolling real-time optimization once every 15 minutes.

**E. COMPARISON OF DIFFERENT SCHEDULING METHODS**

In this section, five optimal scheduling methods are used to evaluate the performance of proposed method in this paper. Cases design of different scheduling methods can be represented as follows:

- Case 1: The proposed method;
- Case 2: Disordered charging;
- Case 3: Optimal scheduling by using time-of-use electricity pricing policy;
- Case 4: Centralized optimization with the target of pursuing the maximum of overall social welfare;
- Case 5: Regardless of the interests of EVA and the EV owners, the goal is to perform peak load shifting.

The objective functions for Case 3-5 are described as follows:

The EVA objective function of Case 3 is consistent with Eq.(9). The only difference is that the time-of-use electricity price is based on the conventional load, which remains unchanged at each time-slot.

The objective function of Case 4 for each time-slot can be described as:

$$\min \sum_{i \in \mathcal{N}} F_{i,t} \tag{20}$$

where  $F_{i,t}$  is consistent with Eq.(9).

The objective function of Case 5 for each time-slot can be described as:

$$\min \sum_{k \in \mathcal{K}} (Q_{total}(k) - Q_{avg,t})^2 \tag{21}$$

$$Q_{avg,t} = \frac{\sum_{k \in \mathcal{K}} Q_{total}(k)}{T - t + 1} \tag{22}$$

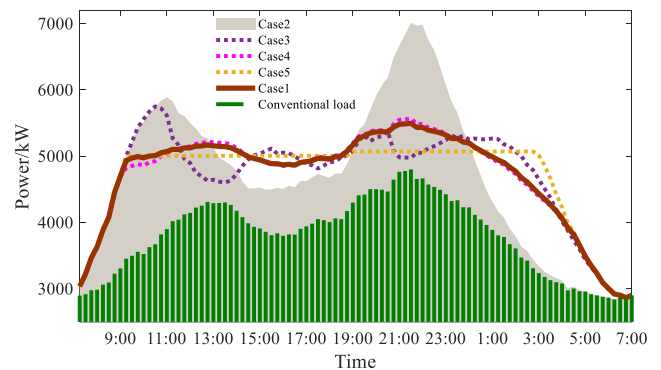


FIGURE 9. Comparison results of different scheduling methods.

The optimization results and the objective function values of different cases are shown in Fig.9 and Table 2, respectively. It can be seen that Case 1, Case 4 and Case 5 can perform the peak load shifting effectively. More importantly, Case 1



**TABLE 2. Objective function values of different scheduling methods.**

Objectives	Total/\$	EVA1/\$	EVA2/\$	EVA3/\$
Case 1	5295.77	1744.36	1750.23	1801.16
Case 2	6074.59	1996.27	2010.27	2068.04
Case 3	5435.10	1788.28	1797.93	1848.89
Case 4	5293.18	1744.5	1748.92	1799.69
Case 5	5432.41	1787.70	1800.30	1844.40

(proposed method) has the best effect. In addition, Case 1 gets the lowest total objective function value except for Case 4, caused by the rational and selfish feature of the EVAs in the game, which indicates that the NE strategy does not lead to the optimal social welfare in the system.

In Case 3, a peak-valley inversion phenomenon occurred between the curve of optimized result and conventional load, which is because the change trend of time-of-use electricity price is consistent with that of conventional load, i.e., the electricity price in the peak period is high, while the electricity price in the valley period is low. Due to the incentive of electricity price, EVAs will adjust the charging plan and concentrate on charging during the valley period. However, since the time-of-use electricity price cannot be adjusted in real-time during each iteration process and there has no direct coordinated scheduling among all EVAs, a large charging peak is generated at the period of low conventional load. Besides, the objective function values of all EVAs are higher than those of Case 1. Therefore, when large-scale EVs are connected to the grid, it is not suitable to use the time-of-use electricity price policy to guide EVAs to make charging plan.

In Case 4, the total objective function value is slightly lower than that of Case 1, which confirms that the NE solution is inconsistent with the optimal solution of the whole social welfare. However, the proposed method (Case 1) is more suitable for multi-player to perform RTOS than the method of Case 4, because of the differences of the objective function of each gaming individual, the rational and selfish characteristics, and the requirement of privacy protection.

Case 5 directly performs peak load shifting by the centralized optimal scheduling. From the results, not only the total objective function value, but also the objective function value of each EVA is higher than those of Case 1. It can be foreseen that all EVAs have more interest to choose the proposed method

In summary, from the DSO's side, the peak load shifting effect of Case 1 is the best, and the total objective function value is just slightly higher than the scheduling Case with the maximum social welfare. Therefore, the proposed method is more suitable for RTOS with large-scale EVs.

#### F. COMPARISON OF DIFFERENT EV ACCESS LEVELS

In this section, different EV access levels are set to evaluate the performance of propose method.

**TABLE 3. Calculating time for different amount of EVs and EVAs.**

Number of EVA	Number of EV	Average calculation time of sub-problem /s	Average calculation time of each period /s
3	1200	0.43	23.45
3	5000	0.46	29.26
3	10000	0.73	35.82
10	10000	0.87	43.92
20	10000	1.06	51.38

It can be seen from Table 3 that the calculation time under all the EV access levels can meet the requirement of engineering practice. As the number of EVAs and EVs participating in the scheduling increases, the algorithm can still maintain good performance in the calculation time. The average calculation time is less than 1 minute. This is because the increase in the number of EVs does not affect the number of variables in the model after adopting EVC method. At the same time, each EVA adopts distributed parallel computing, so the increase in the number of EVAs does not have a large impact on the time for each iteration. If a more computationally efficient device is used, the calculation time can be further reduced. Therefore, the scheduling architecture and algorithm proposed in this paper are suitable and can effectively solve the RTOS problem with large-scale EVs.

#### VI. CONCLUSION

This paper proposes a large-scale EVs real-time optimal scheduling based on dynamic non-cooperative game approach and proves the existence and uniqueness of NE solution of dynamic game model, and uses ADMM algorithm to achieve distributed solving. Simulation cases show that:

- 1) The proposed model with dynamic electricity price scheme effectively achieves load-flattening and reduces charging cost of EVAs effectively.
- 2) The centralized optimization model is decomposed and solved by ADMM algorithm to achieve distributed computing. Thus, the proposed method can protect the information security of each EVA and reduce the possibility of information leakage.
- 3) By comparing the optimization results with different number of EVs, the proposed method is robust and obtains the optimal solution quickly. The feasibility of the model in practical application is demonstrated, which is suitable for solving the real-time scheduling problem of large-scale EV access.

In this paper, the interaction mechanism is limited to among DSO and EVAs. Designing a bilevel game which accounts the interests of DSO, EVA and EV owners and its own solution method or artificial intelligence method [34] are the focus in future study.

#### APPENDIX A PROOF OF THE CORRECTNESS OF THE POTENTIAL FUNCTION

From the potential game theory and the Eq. (16), it can be seen that the proof that the constructed potential function (17)

satisfies the potential game theory is equivalent to:

$$\nabla_{x_i(t)} P(x(t)) = \nabla_{x_i(t)} F_i(x(t)) \quad (23)$$

Among them,  $\nabla$  is the gradient operator; in this problem,  $x_i(t)$  is  $Q_i(t)$ ; that is, only the proof is required. For any  $Q_i(t)$ ,  $t \in T$ , the following formula holds:

$$\frac{\partial P(x(t))}{\partial Q_i(t)} = \frac{\partial F_i(x(t))}{\partial Q_i(t)} \quad (24)$$

Since  $P_1(x_i(t))$  the part of the potential function  $P(x_i(t))$  that represents the satisfaction is consistent with the part of the EVA optimization target that satisfies the satisfaction degree, the result of the part is still equal after the derivation. Therefore, it is only necessary to prove that for any  $Q_i(t)$ ,  $t \in T$ , the following formula holds:

$$\frac{\partial P_2(x(t))}{\partial Q_i(t)} = \frac{\partial}{\partial Q_i(t)} \left[ \sum_{k \in T_k} C_i(k) \right] \quad (25)$$

The left side of the equation:

$$\frac{\partial P_2(x(t))}{\partial Q_i(t)} = \delta(t)Q_{load}(t) + 2\delta(t)Q_i(t) + \sum_{j \in N, j \neq i} \delta(t)Q_j(t) \quad (26)$$

The right side of the equation:

$$\begin{aligned} & \frac{\partial}{\partial Q_i(t)} \left[ \sum_{k \in T_k} C_i(k) \right] \\ &= \delta(t) \frac{\partial Q_{total}(t)}{\partial Q_i(t)} Q_i(t) + \delta(t)Q_{total}(t) \\ &= \delta(t)Q_i(t) + \delta(t)(Q_{load}(t) + Q_{sum}(t)) \\ &= \delta(t)Q_{load}(t) + 2\delta(t)Q_i(t) + \sum_{j \in N, j \neq i} \delta(t)Q_j(t) \end{aligned} \quad (27)$$

The equations are equal on both sides. Therefore, the function  $P(x(t))$  is the potential function of each EVA game.

### APPENDIX B PROOF OF THE POTENTIAL FUNCTION IS CONVEX AND FEASIBLE SPACE IS CONVEX

For the potential function  $P(x(t))$ ,  $P_1(x(t))$  and  $P_2(x(t))$  can be separated for analysis.

For  $P_1(x(t))$ , it can be known from Eq. (6)-(8) that  $P_1(x(t))$  is composed of a series of convex quadratic functions, and it is easy to know that  $P_1(x(t))$  is a convex function.

For  $P_2(x(t))$ , calculate the Hessian matrix of  $P_2(x(t))$  due to

$$\frac{\partial^2 P_2(x(t))}{\partial Q_i^2(t)} = 2\delta(t) \frac{\partial^2 P_2(x(t))}{\partial Q_i(t) \partial Q_j(t)} = \delta(t) \quad (28)$$

Therefore, the Hessian matrix of the potential functions with N EVA participating games can be expressed as follows:

$$A = \begin{bmatrix} 2\delta(t) & \delta(t) & \cdots & \delta(t) \\ \delta(t) & 2\delta(t) & \cdots & \delta(t) \\ \vdots & \vdots & \ddots & \vdots \\ \delta(t) & \delta(t) & \cdots & 2\delta(t) \end{bmatrix}_{N \times N} \quad (29)$$

The eigenvalues of the Hessian matrix can be calculated:  $\lambda_1 = (N + 1)\delta(t)$ ,  $\lambda_2, \lambda_3, \dots, \lambda_N = \delta(t)$ ; when  $\delta(t) > 0$  all eigenvalues are greater than 0 and the Hessian matrix is positive, the provable function  $P_2(x(t))$  can be proof to be a convex function.

In summary, the potential function  $P(x(t))$  is a convex function. In addition, the constraints on the feasible domain  $x_i(t)$  are linear functions, and it is easy to know that the feasible domain  $x_i(t)$  is a convex set.

### APPENDIX C DISTRIBUTED OPTIMIZATION TARGET DECOMPOSITION PROCESS

$$\begin{aligned} P_1(x(t_k)) &= - \sum_{i \in N} \sum_{k \in T_k} U_i(k) \\ &= - \sum_{k \in T_k} (U_1(k) + U_2(k) + \cdots + U_N(k)) \quad (30) \\ P_2(x(t_k)) &= \sum_{i \in N} \left[ \sum_{k \in T_k} \left( \delta(k)Q_{load}(k)Q_i(k) + \delta(k)Q_i^2(k) \right. \right. \\ & \quad \left. \left. + \sum_{i < j \in N} \delta(k)Q_i(k)Q_j(k) \right) \right] \\ &= \frac{1}{2} \delta(k) \sum_{k \in T_k} \left( \begin{aligned} & Q_1^2(k) + Q_1^2(k) + Q_1(k)Q_2(k) \\ & + \cdots + Q_1(k)Q_N(k) + \\ & Q_2^2(k) + Q_2(k)Q_1(k) + Q_2^2(k) \\ & + \cdots + Q_2(k)Q_N(k) + \\ & \vdots \\ & Q_N^2(k) + Q_N(k)Q_1(k) \\ & + Q_N(k)Q_2(k) + \cdots + Q_N^2(k) \end{aligned} \right) \\ & \quad + \frac{1}{2} \delta(k) \sum_{k \in T_k} \left( \begin{aligned} & 2Q_{load}(k)Q_1(k) + \\ & 2Q_{load}(k)Q_2(k) + \\ & \vdots \\ & 2Q_{load}(k)Q_N(k) \end{aligned} \right) \\ &= \frac{1}{2} \delta(k) \sum_{k \in T_k} \left( \begin{aligned} & Q_1(k)Q_{sum}(k) + \\ & Q_2(k)Q_{sum}(k) + \\ & \vdots \\ & Q_N(k)Q_{sum}(k) \end{aligned} \right) \\ & \quad + \frac{1}{2} \delta(k) \sum_{k \in T_k} \left( Q_1^2(k) + Q_2^2(k) + \cdots + Q_N^2(k) \right) \\ & \quad + \delta(k) \sum_{k \in T_k} Q_{load}(k)Q_{sum}(k) \\ &= \frac{1}{2} \delta(k) \sum_{k \in T_k} Q_{sum}^2(k) \\ & \quad + \frac{1}{2} \delta(k) \sum_{k \in T_k} \left( Q_1^2(k) + Q_2^2(k) + \cdots + Q_N^2(k) \right) \\ & \quad + \delta(k) \sum_{k \in T_k} Q_{load}(k)Q_{sum}(k) \quad (31) \end{aligned}$$

$$\begin{aligned}
P(x(t_k)) &= P_1(x(t_k)) + P_2(x(t_k)) \\
&= \frac{1}{2} \delta(k) \sum_{k \in T_k} Q_{\text{sum}}^2(k) + \delta(k) \sum_{k \in T_k} Q_{\text{load}}(k) Q_{\text{sum}}(k) \\
&\quad + \frac{1}{2} \delta(k) \sum_{k \in T_k} (Q_1^2(k) + Q_2^2(k) + \dots + Q_N^2(k)) \\
&\quad - \sum_{k \in T_k} (U_1(k) + U_2(k) + \dots + U_N(k)) \\
&= W_1(Q_{\text{sum}}) + W_2(Q_1, U_1) \\
&\quad + W_2(Q_2, U_2) + \dots + W_2(Q_N, U_N) \quad (32)
\end{aligned}$$

## REFERENCES

- [1] P. Denholm and W. Short, "Evaluation of utility system impacts and benefits of optimally dispatched plug-in hybrid electric vehicles (revised)," NREL, Golden, CO, USA, Tech. Rep. NREL/TP-620-40293, Oct. 2006.
- [2] K. Clement-Nyns, E. Haesen, and J. Driesen, "The impact of charging plug-in hybrid electric vehicles on a residential distribution grid," *IEEE Trans. Power Syst.*, vol. 25, no. 1, pp. 371–380, Feb. 2010, doi: 10.1109/TPWRS.2009.2036481.
- [3] S. W. Hadley and A. A. Tsvetkova, "Potential impacts of plug-in hybrid electric vehicles on regional power generation," *Electr. J.*, vol. 22, no. 10, pp. 56–68, Dec. 2009, doi: 10.1016/j.tej.2009.10.011.
- [4] IEA Publications. (2019). *Global EV Outlook 2019: Scaling-Up the Transition to Electric Mobility*. [Online]. Available: <https://webstore.iea.org/global-ev-outlook-2019>
- [5] S. K. Injeti and V. K. Thunuguntla, "Optimal integration of DGs into radial distribution network in the presence of plug-in electric vehicles to minimize daily active power losses and to improve the voltage profile of the system using bio-inspired optimization algorithms," *Protection Control Modern Power Syst.*, vol. 5, no. 1, pp. 21–35, Dec. 2020, doi: 10.1186/s41601-019-0149-x.
- [6] L. Xi, L. Zhang, J. Liu, Y. Li, X. Chen, L. Yang, and S. Wang, "A virtual generation ecosystem control strategy for automatic generation control of interconnected microgrids," *IEEE Access*, vol. 8, pp. 94165–94175, 2020, doi: 10.1109/ACCESS.2020.2995614.
- [7] Z. Huang, B. Fang, and J. Deng, "Multi-objective optimization strategy for distribution network considering V2G-enabled electric vehicles in building integrated energy system," *Protection Control Modern Power Syst.*, vol. 5, no. 1, pp. 48–55, Dec. 2020, doi: 10.1186/s41601-020-0154-0.
- [8] S. Deilami, A. S. Masoum, P. S. Moses, and M. A. S. Masoum, "Real-time coordination of plug-in electric vehicle charging in smart grids to minimize power losses and improve voltage profile," *IEEE Trans. Smart Grid*, vol. 2, no. 3, pp. 456–467, Sep. 2011, doi: 10.1109/TSG.2011.2159816.
- [9] W. Jiang and Y. Zhen, "A real-time EV charging scheduling for parking lots with PV system and energy store system," *IEEE Access*, vol. 7, pp. 86184–86193, Jul. 2019, doi: 10.1109/ACCESS.2019.2925559.
- [10] S. I. Vagropoulos, D. K. Kyriazidis, and A. G. Bakirtzis, "Real-time charging management framework for electric vehicle aggregators in a market environment," *IEEE Trans. Smart Grid*, vol. 7, no. 2, pp. 948–957, Mar. 2016, doi: 10.1109/TSG.2015.2421299.
- [11] S. Bashash and H. K. Fathy, "Cost-optimal charging of plug-in hybrid electric vehicles under time-varying electricity price signals," *IEEE Trans. Intell. Transp. Syst.*, vol. 15, no. 5, pp. 1958–1968, Oct. 2014, doi: 10.1109/TITS.2014.2308283.
- [12] L. Yang, J. Zhang, and H. V. Poor, "Risk-aware day-ahead scheduling and real-time dispatch for electric vehicle charging," *IEEE Trans. Smart Grid*, vol. 5, no. 2, pp. 693–702, Mar. 2014, doi: 10.1109/TSG.2013.2290862.
- [13] H. Wang, Z. Lei, X. Zhang, B. Zhou, and J. Peng, "A review of deep learning for renewable energy forecasting," *Energy Convers. Manage.*, vol. 198, Oct. 2019, Art. no. 111799, doi: 10.1016/j.enconman.2019.111799.
- [14] S. Vandael, B. Claessens, M. Hommelberg, T. Holvoet, and G. Deconinck, "A scalable three-step approach for demand side management of plug-in hybrid vehicles," *IEEE Trans. Smart Grid*, vol. 4, no. 2, pp. 720–728, Jun. 2013, doi: 10.1109/TSG.2012.2213847.
- [15] Z. Xu, W. Su, Z. Hu, Y. Song, and H. Zhang, "A hierarchical framework for coordinated charging of plug-in electric vehicles in China," *IEEE Trans. Smart Grid*, vol. 7, no. 1, pp. 428–438, Jan. 2016, doi: 10.1109/TSG.2014.2387436.
- [16] Z. Liu, Q. Wu, M. Shahidehpour, C. Li, S. Huang, and W. Wei, "Transactive real-time electric vehicle charging management for commercial buildings with PV on-site generation," *IEEE Trans. Smart Grid*, vol. 10, no. 5, pp. 4939–4950, Sep. 2019, doi: 10.1109/TSG.2018.2871171.
- [17] Z. Liu, Q. Wu, K. Ma, M. Shahidehpour, Y. Xue, and S. Huang, "Two-stage optimal scheduling of electric vehicle charging based on transactive control," *IEEE Trans. Smart Grid*, vol. 10, no. 3, pp. 2948–2958, May 2019, doi: 10.1109/TSG.2018.2815593.
- [18] Z. Pan, T. Yu, J. Li, K. Qu, L. Chen, B. Yang, and W. Guo, "Stochastic transactive control for electric vehicle aggregators coordination: A decentralized approximate dynamic programming approach," *IEEE Trans. Smart Grid*, early access, May 6, 2020, doi: 10.1109/TSG.2020.2992863.
- [19] A. Y. Saber and G. K. Venayagamoorthy, "Resource scheduling under uncertainty in a smart grid with renewables and plug-in vehicles," *IEEE Syst. J.*, vol. 6, no. 1, pp. 103–109, Mar. 2012, doi: 10.1109/JSYST.2011.2163012.
- [20] M. S. Kuran, A. Carneiro Viana, L. Iannone, D. Kofman, G. Mermoud, and J. P. Vasseur, "A smart parking lot management system for scheduling the recharging of electric vehicles," *IEEE Trans. Smart Grid*, vol. 6, no. 6, pp. 2942–2953, Nov. 2015, doi: 10.1109/TSG.2015.2403287.
- [21] H. Rashidzadeh-Kermani, H. Najafi, A. Anvari-Moghaddam, and J. Guerrero, "Optimal decision-making strategy of an electric vehicle aggregator in short-term electricity markets," *Energies*, vol. 11, no. 9, p. 2413, Sep. 2018, doi: 10.3390/en11092413.
- [22] J. C. Mukherjee and A. Gupta, "A review of charge scheduling of electric vehicles in smart grid," *IEEE Syst. J.*, vol. 9, no. 4, pp. 1541–1553, Dec. 2015, doi: 10.1109/JSYST.2014.2356559.
- [23] W. Tushar, W. Saad, H. V. Poor, and D. B. Smith, "Economics of electric vehicle charging: A game theoretic approach," *IEEE Trans. Smart Grid*, vol. 3, no. 4, pp. 1767–1778, Dec. 2012, doi: 10.1109/TSG.2012.2211901.
- [24] H. Yang, X. Xie, and A. V. Vasilakos, "Noncooperative and cooperative optimization of electric vehicle charging under demand uncertainty: A robust stackelberg game," *IEEE Trans. Veh. Technol.*, vol. 65, no. 3, pp. 1043–1058, Mar. 2016, doi: 10.1109/TVT.2015.2490280.
- [25] L. Zhang and Y. Li, "A game-theoretic approach to optimal scheduling of parking-lot electric vehicle charging," *IEEE Trans. Veh. Technol.*, vol. 65, no. 6, pp. 4068–4078, Jun. 2016, doi: 10.1109/TVT.2015.2487515.
- [26] H. Wang, Y. Liu, B. Zhou, C. Li, G. Cao, N. Voropai, and E. Barakhtenko, "Taxonomy research of artificial intelligence for deterministic solar power forecasting," *Energy Convers. Manage.*, vol. 214, Jun. 2020, Art. no. 112909, doi: 10.1016/j.enconman.2020.112909.
- [27] H. Z. Wang, G. B. Wang, G. Q. Li, J. C. Peng, and Y. T. Liu, "Deep belief network based deterministic and probabilistic wind speed forecasting approach," *Appl. Energy*, vol. 182, pp. 80–93, Nov. 2016, doi: 10.1016/j.apenergy.2016.08.108.
- [28] Z. N. Pan, T. Yu, L. P. Chen, B. Yang, B. Wang, and W. X. Guo, "Real-time stochastic optimal scheduling of large-scale electric vehicles: A multidimensional approximate dynamic programming approach," *Int. J. Electr. Power Energy Syst.*, vol. 116, Mar. 2020, Art. no. 105542, doi: 10.1016/j.ijepes.2019.105542.
- [29] S. Bahrami, M. Toulabi, S. Ranjbar, M. Moeini-Aghtaie, and A. M. Ranjbar, "A decentralized energy management framework for energy hubs in dynamic pricing markets," *IEEE Trans. Smart Grid*, vol. 9, no. 6, pp. 6780–6792, Nov. 2018, doi: 10.1109/TSG.2017.2723023.
- [30] D. Monderer and L. S. Shapley, "Potential games," *Games Econ. Behav.*, vol. 14, no. 1, pp. 3124–3143, May 1996, doi: 10.1006/game.1996.0044.
- [31] J. Li, C. Li, Y. Xu, Z. Y. Dong, K. P. Wong, and T. Huang, "Noncooperative game-based distributed charging control for plug-in electric vehicles in distribution networks," *IEEE Trans. Ind. Informat.*, vol. 14, no. 1, pp. 301–310, Jan. 2018, doi: 10.1109/TII.2016.2632761.
- [32] D. Xu, Q. Wu, B. Zhou, C. Li, L. Bai, and S. Huang, "Distributed multi-energy operation of coupled electricity, heating and natural gas networks," *IEEE Trans. Sustain. Energy*, early access, Dec. 23, 2019, doi: 10.1109/TSTE.2019.2961432.
- [33] M. Kranning, E. Chu, J. Lavaei, and S. Boyd, "Message passing for dynamic network energy management," in *Dynamic Network Energy Management via Proximal Message Passing*. Boston, MA, USA: Now, 2014. [Online]. Available: <https://ieeexplore.ieee.org/document/8187254>
- [34] L. Xi, L. Yu, Y. Xu, S. Wang, and X. Chen, "A novel multi-agent DDQN-AD method-based distributed strategy for automatic generation control of integrated energy systems," *IEEE Trans. Sustain. Energy*, early access, Dec. 9, 2019, doi: 10.1109/TSTE.2019.2958361.



**LVPENG CHEN** received the B.Eng. degree in electrical engineering from the South China University of Technology, Guangzhou, China, in 2017, where he is currently pursuing the M.S. degree in electrical engineering with the College of Electric Power. His research interests include power systems operation and power load forecasting.



**WEILING GUAN** received the B.Eng. degree in electrical engineering from the South China University of Technology, Guangzhou, China, in 2018, where he is currently pursuing the M.S. degree in electrical engineering with the College of Electric Power. His research interests include power system demand response and power system planning.



**TAO YU** (Member, IEEE) received the B.Eng. degree in electrical power systems from Zhejiang University, Hangzhou, China, in 1996, the M.Eng. degree in hydroelectric engineering from Yunnan Polytechnic University, Kunming, China, in 1999, and the Ph.D. degree in electrical engineering from Tsinghua University, Beijing, China, in 2003. He is currently a Professor of power systems with the School of Electric Power, South China University of Technology, Guangzhou, China. His special fields of interest include nonlinear and coordinated control theory, artificial intelligence techniques in planning, and the operation of power systems.



**YING SHI** received the B.Eng. degree in electrical engineering from the South China Agricultural University, Guangzhou, China, in 2017. He is currently pursuing the M.S. degree in electrical engineering with the College of Electric Power, South China University of Technology, Guangzhou, China. His research interests include optimization and data mining of power and energy systems.



**YONGXIANG CHEN** received the B.Eng. degree in electrical engineering from the South China University of Technology, Guangzhou, China, in 2018, where he is currently pursuing the M.S. degree in electrical engineering with the College of Electric Power. His research interests include power system demand response and power system planning.



**ZHENNING PAN** received the B.Eng. degree in electrical engineering from the South China University of Technology, Guangzhou, China, in 2016, where he is currently pursuing the Ph.D. degree in electrical engineering with the College of Electric Power. His major research interests include intelligent optimization and machine learning in the operation of power systems.

...